Theoretical study of the adsorption of histidine amino acid on graphene

S J Rodríguez[1], L Makinistian[2] and E Albanesi[1]

[1]IFIS-CONICET, Güemes 3450, 3000 Santa Fe, Argentina and Facultad de Ingeniería, Universidad Nacional de Entre Ríos, 3101 Oro Verde (ER), Argentina

[2]Departamento de Física, e Instituto de Física Aplicada (INFAP), Universidad Nacional de San Luis-CONICET, Ejército de los Andes 950, D5700BWS San Luis, Argentina

E-mail: sindy.rodriguez@santafe-conicet.gov.ar

Abstract. Previous studies have demonstrated how the interactions between biomolecules and graphene play a crucial role in the characterization and functionalization of biosensors. In this paper we present a theoretical study of the adsorption of histidine on graphene using density functional theory (DFT). In order to evaluate the relevance of including the carboxyl (-COOH) and amino (-NH$_2$) groups in the calculations, we considered i) the histidine complete (i.e., with its carboxyl and its amino groups included), and ii) the histidine's imidazole ring alone. We calculated the density of states for the two systems before and after adsorption. Furthermore, we compared the results of three approximations of the exchange and correlation interactions: local density (LDA), the generalized gradients by Perdew, Burke and Ernzerhof (GGA-PBE), and one including van der Waals forces (DFT-D2). We found that the adsorption energy calculated by DFT-D2 is higher than the other two: $E_{ads-DFT-D2} > E_{ads-LDA} > E_{ads-GGA}$. We report the existence of charge transfer from graphene to the molecule when the adsorption occurs; this charge transfer turns up to be greater for the complete histidine than for the imidazole ring alone. Our results revealed that including the carboxyl and amino groups generates a shift in the states of imidazole ring towards E_F.

1. Introduction

Graphene is a two-dimensional crystal with special chemical and physical properties [1, 2]. Consequently, since its discovery, it has been used in fields such as electronics, biomedicine, biotechnology and pharmacology, among others [3, 4, 5]. For instance, Wang *et al.* [6], in the area of drug delivery devices and molecular transport, reported that graphene could be used as a good vehicle of DNA aptamers into living cells, because it provides effective protection of the oligonucleotides from enzymatic cleavage. Furthermore, Hess *et al.* [7, 8] developed graphene transistor arrays for recording cellular action potentials, which have applications in neural prosthesis. The study suggests the simple integration of graphene electronics with flexible technologies (an important aspect of biomedical implants design), because they prevent severe tissue damage [7].

In the area of molecular biology and nanomaterials, different studies have been developed on the adsorption of biological molecules on graphene sheets and carbon nanotubes [9, 10, 11, 12]. Graphene sensors can provide high sensitivity, selectivity and low intrinsic electronic noise, which is a great advantage over other materials [3]. Chemical sensors of carbon nanotubes for small

molecules such as NO_2, NH_3, O_2 and H_2 have been tested experimentally and the graphene electronic structure shows high sensitivity when different molecules are adsorbed [13, 14].

Theoretical works use first-principles calculations to analyze the nature of the interactions between biomolecules and graphene [15, 16, 17]. For example, Gowtham *et al.* [11, 18], using DFT-LDA and $Møller - Plesset$ second-order perturbation theory (MP2), investigated the interaction of the nucleobases adenine (A), cytosine (C), guanine (G), thymine (T), and uracil (U) with graphene, demonstrating that they exhibit significantly different interaction strengths when physisorbed on graphene. With a similiar approach, Rajesh *et al.* [9] reported significant differences in the binding strength between aromatic rings of amino acids phenylalanine, histidine, tyrosine and tryptophan with graphene (and also with single-walled carbon nanotubes), suggesting once again the potential use of graphene as a selective biosensor. As Gowtham *et al.* [11] and Rajesh *et al.* [9] mentioned, the details of the interaction between DNA, proteins and amino acids with graphene —and carbon nanotubes— have not been fully understood. In this work, theoretical results based on DFT for the adsorption of histidine on graphene are presented. Two adsorbates were considered (both on an infinite graphene sheet): histidine with its -COOH and $-NH_2$ groups, and the imidazole ring alone. The discussion focused on: i) comparing the results of three approximations to the exchange and correlation interactions —LDA, GGA-PBE and DFT-D2—, ii) evaluating the relevance of including the carboxyl and amino groups in the calculations (relevance that, to the best of our knowledge, has not been reported in the literature). Equilibrium configurations for each system, energies and adsorption distances, densities of states and net charge transfer are presented.

2. Computational Details

The *ab initio* calculations were developed in the formalism of DFT using the OpenMX package [19]. Numerical pseudo-atomic orbitals (PAOs) were used as basis function to expand one-particle Kohn-Sham wave functions. The PAO were specified by H5.0-s1, C5.0-s2p2d1, O6.0-s2p2d1, N6.0-s2p2d1, where H, C, O and N are the atomic symbols, 5.0 and 6.0 represent the cutoff radius (Bohr) in the generation by the confinement scheme [20, 21], and s2p2d1, for example, indicates the employment of two primitive orbitals for each of the s and p components and one primitive orbital for the d component.

In studies on the interaction between simple benzene derivatives with graphene, graphite and carbon nanotubes, the LDA approximation correctly described the electronic structure and adsorption geometry (comparison between adsorption-energy DFT descriptions of graphite and the experimental thermal desorption energy) [17]. Furthermore, adsorption calculations of DNA nucleobases on graphene by Lee *et al.* [15], and of adenine on graphite by Ortmann *et al.* [16] suggest that the GGA-PBE approximation does not accurately represent the $\pi - \pi$ bonds in the graphene molecule interface, resulting in low energy bonds and high adsorption distances. LDA, on the other hand, improves adsorption distances, approximating better to experimental values and DFT corrections including van der Waals interactions [11]. With the aim of contributing in this aspects, we studied the adsorption of histidine on graphene using three approximations: local LDA, generalized gradients GGA-PBE [22], and van der Waals DFT-D2 [23].
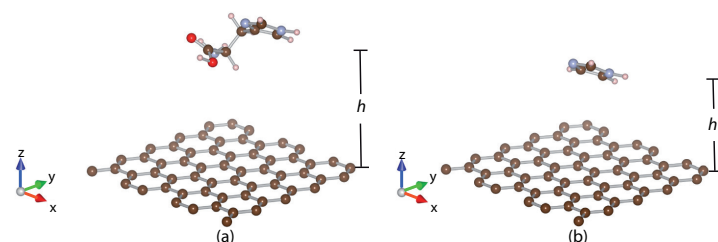

Figure 1. (a) Histidine with -COOH and $-NH_2$ groups on graphene. (b) Histidine imidazole ring on graphene.

The system was modelled with an orthorhombic supercell of $12.78 \times 12.29 \times 25.00$ Å^3 (these dimensions are sufficient to uncouple the graphene sheets and avoid interactions between molecules of adjacent cells); an energy cut-off of 180 Ry and a k-mesh of $5 \times 5 \times 1$ for the SCF, with a refinement up to $50 \times 50 \times 1$ for DOS calculations; and, for geometry optimization, the convergence criterion was set to 0.02 eV/Å for histidine with -COOH and -NH$_2$, and 0.015 eV/Å for the imidazole ring. The graphene sheet was located at the bottom of the cell as shown in Fig. 1.

Initially we located the molecule at distance h from graphene, far enough from it, so a reference energy decoupled (E_{ref}) could be determined for the latter calculation of the interaction energy (attraction, or rejection if too close): $E_{int}(h) = E_{tot}(h)-E_{ref}$, where $E_{ref} = E_{tot}(h=12.5$ Å). The adsorption energy E_{ads} is that of the interaction at the global minimum of the curves $E_{int}(h)$ in Fig. 2. In order to determine the adsorption energy and the mean final distance of the biomolecule to the graphene sheet, two relaxations were performed. In the first relaxation we considered the molecule alone. Subsequently, the relaxed molecule was placed at several heights from the graphene sheet. For each height considered, a second relaxation for all atoms (histidine and graphene sheet) was performed. Once the adsorbate-substrate system was relaxed, the final average distance (measured from the geometric center of the biomolecule to the graphene sheet) and the interaction energy were obtained.

3. Results and Discussion

We begin by describing the equilibrium structures for the two systems considered (for LDA, GGA-PBE and DFT-D2). These results are shown in Fig. 2, from where it is clear that the interaction is negligible for distances greater than 6 Å . Table 1 displays the vertical distances between the molecule and the graphene sheet, and the corresponding adsorption energies, for each of the three exchange and correlation schemes used. For the two systems, we find that $E_{ads-DFT-D2} > E_{ads-LDA} > E_{ads-GGA}$. The GGA-PBE approximation resulted in very low adsorption energies and relatively long distances between substrate-adsorbate, which clearly indicates that it does not correctly describe the π-π interactions. The results for LDA and DFT-D2 are relatively close to each other. There is a strong physisorption between histidine and graphene, when considering van der Waals interactions. The adsorption energies are improved in the systems studied when the DFT-D2 scheme is performed—because it includes long-range forces—. This coincides with results for adsorption of nucleotides [15].
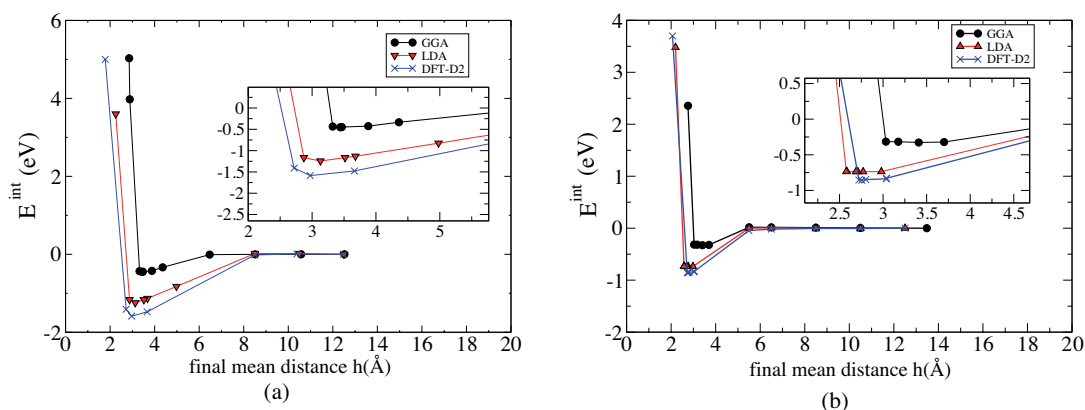

Figure 2. Interaction energy vs. mean distance between the graphene sheet and the histidine with (a), and without (b) the -COOH and -NH$_2$ groups.

Table 1. Theoretical results of adsorption energy for exchange and correlation approaches LDA, GGA-PBE and DFT-D2. d_{ads}^{His-Gr} is the distance measured between the geometric center of the biomolecule and graphene sheet. In Ref. [24]. hybrid meta exchange- correlation functionals called M06- 2X/6-311G (Gaussian 09). In Ref. [25] hybrid meta exchange-correlation functional, called M05-2X (Gaussian 09). No experimental results are available for these systems.

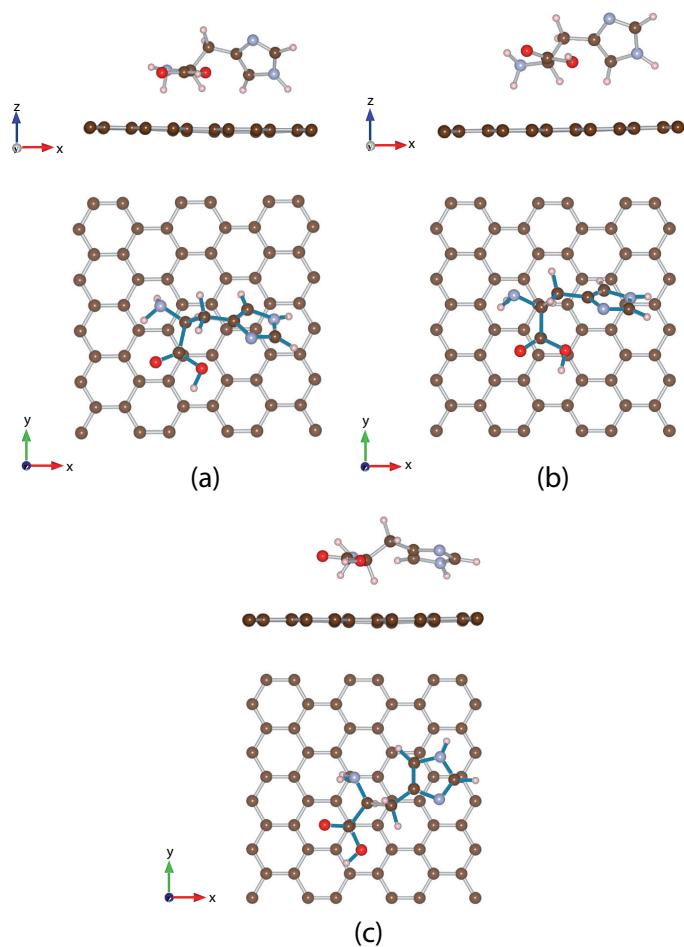| Approx.	System	This Work		Other work	
		E_{ads} (eV)	d_{ads}^{His-Gr} Å	E_{ads} (eV)	d_{cell} Å
LDA	Histidine	1.24	3.13	—	—
	Imidazole ring	0.73	2.77	—	—
GGA-PBE	Histidine	0.45	3.44	—	—
	Imidazole ring	0.32	3.41	0.21(0.55) [9]	3.21 [9]
DFT-D2	Histidine	1.58	2.97	—	—
	Imidazole ring	0.85	2.90	—	—
Other	Histidine	—	—	0.77 [24]	3.195 [24]
	Imidazole ring	—	—	0.14 [25]	3.38 [25]

Figure 3. Equilibrium geometry for histidine with -COOH and -NH$_2$ groups on graphene. (a) LDA (b) GGA-PBE (c) DFT-D2.
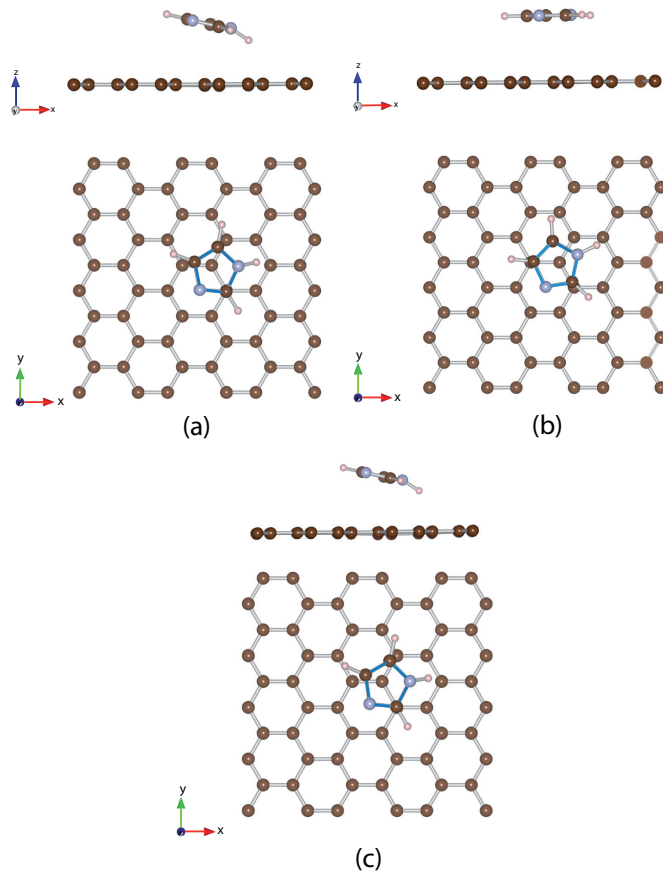
Figure 4. Equilibrium geometry for imidazole ring on graphene. (a) LDA (b) GGA-PBE (c) DFT-D2.

Equilibrium geometries are shown in Fig. 3 and Fig. 4. The equilibrium configurations for the imidazole ring show that the molecule is oriented parallel to the graphene sheet in GGA-PBE, while the ring has a slight angle in the LDA and DFT-D2 approximations. The histidine with the carboxyl and amino groups did not displayed a parallel orientation of the ring, however, when including van der Waals interactions, the ring of the molecule tends to be more parallel to the graphene sheet, see Fig. 3(c).

In order to study the possibility of using graphene as a sensor for histidine, we calculated the DOS for: histidine alone —with and without carboxyl and amine groups—, graphene alone, histidine on graphene, imidazole ring on graphene, and histidine on graphene including the individual contribution of the -COOH and -NH$_2$ groups, and the imidazole ring (see Fig. 5). Figure 5(a) displays the well known zero gap DOS of pure graphene. Figures 5(b)(c) and (d) show a typical molecular DOS with many very sharp peaks (as expected, there are more peaks for histidine with carboxyl and amine groups). Figures 5(e)(f) and (g) clearly show how the presence of the carboxyl and the amino groups produces significant differences. In particular, it is to be remarked that the peaks that lay closer to E$_F$ (in the valence band) are indeed due to the imidazole ring, see Fig. 5(h). However when the -COOH and -NH$_2$ groups are included the states are shifted closer to E$_F$ —first peak in the valence band, blue curve, see arrow—. If van der Waals forces are considered the shifting of that first peak is 0.29 eV towards E$_F$.

With regards to the three approaches: GGA-PBE and DFT-D2 show slight differences, while LDA is sensibly different from the other two (the positions and the heights of the peaks). The peaks marked with arrows in Figs. 5(e)(f) and (g) for histidine and imidazole ring respectively, lay at, LDA: -0.76 eV and -1.67 eV; GGA-PBE: -1.33 eV and -1.89 eV; DFT-D2: -1.24 eV and

-1.53 eV.

Including the carboxyl and amino groups should be of great importance in studies of electronic transport in graphene, since their presence implies more states available near the Fermi energy that can move from the valence band to the conduction band. Furthermore, the shift of states of the imidazole ring towards E_F that appears when the carboxyl and amino groups are included, could improve the sensitivity of a graphene-based sensor upon the application of a bias voltage.

In all systems studied, no gap opening is observed after the adsorption, so that the molecule-graphene system retains the semi-metallic character of pure graphene.
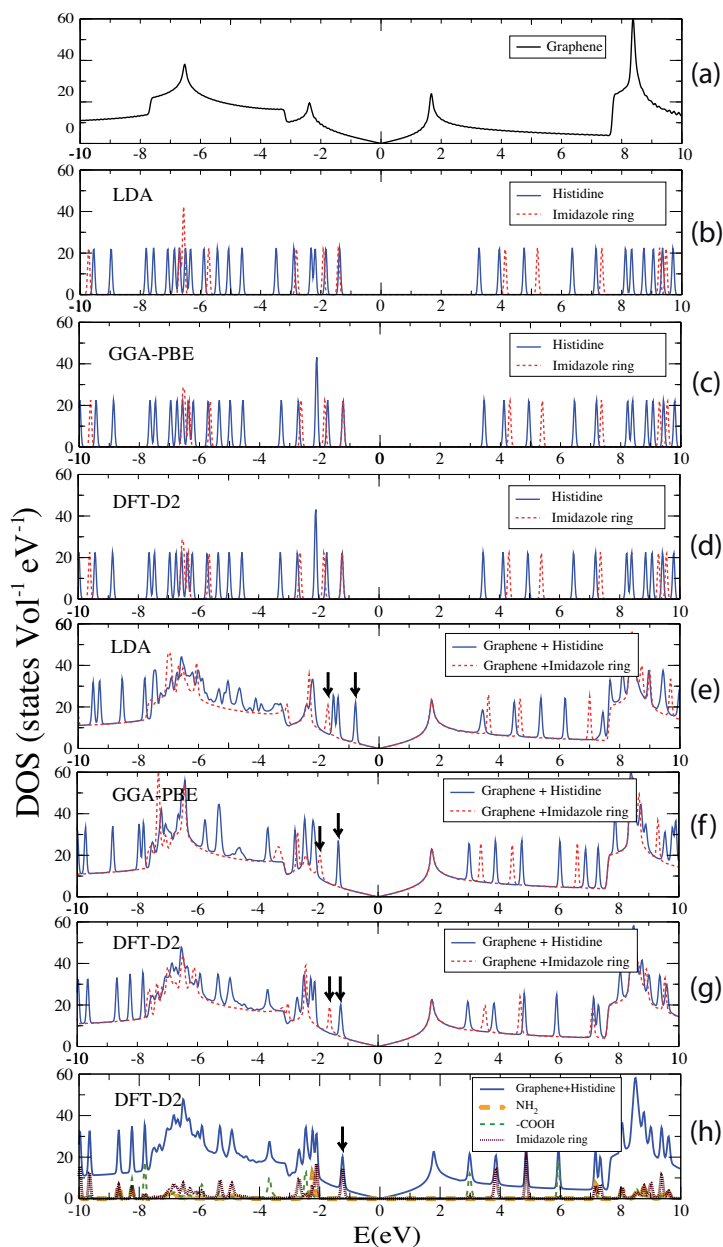

Figure 5. Total DOS of (a) pristine graphene, (b)(c)(d) histidine and imidazole ring, (e)(f)(g) histidine on graphene —with and without carboxyl and amine groups—, and (h) histidine on graphene, including DOS for -COOH, -NH$_2$ and imidazole ring separately.

The charge density of graphene plus histidine with carboxyl and amine groups, gives a qualitative measure of the adsorption-induced charge redistribution. In Fig. 6 we present the charge density for two planes in the direction [001], in (a) the adsorbate-substrate interaction is

negligible and the charge distribution is uniform for each carbon atom of the graphene sheet. In Fig. 6(b) the charge density for graphene after the adsorption process is displayed: changes of charge distribution are more remarkable to the carbon atoms that are under the molecule, see Fig. 6(c). The analysis of the Mulliken charges in the calculations shows a very small charge transfer. We report the existence of a charge transfer from the graphene sheet to the molecule, see Table 2. For the three approaches, the charge transfer is higher when the groups -COOH and -NH$_2$ are considered. Again, we find that including them in the calculations is a relevant aspect of the functionalization and characterization of graphene as a biosensor: a greater charge transfer could be significant regarding electronic transport through the histidine-graphene system.
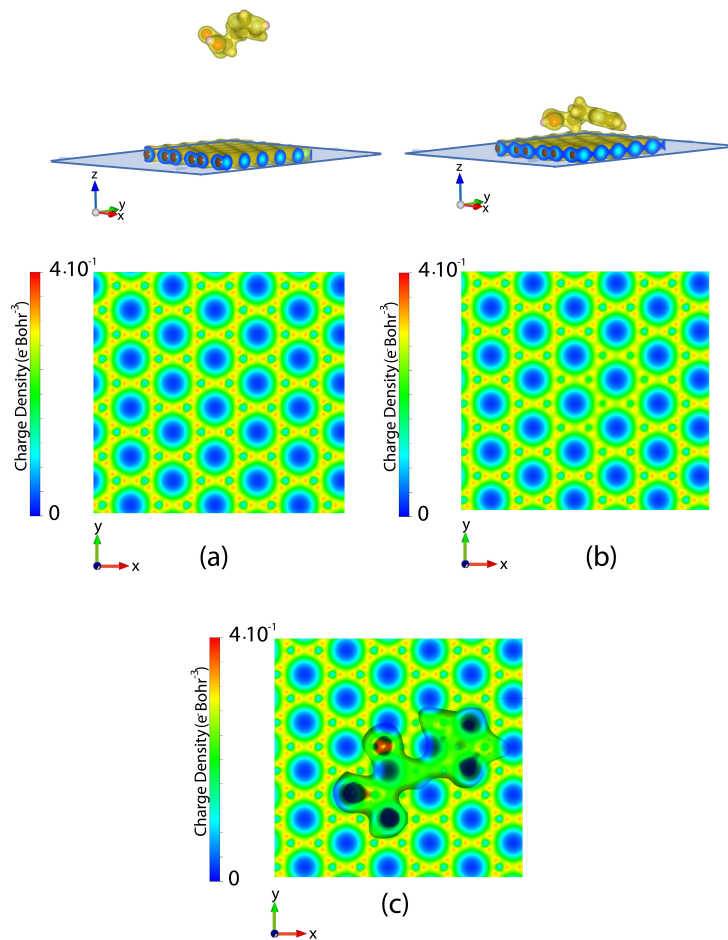

Figure 6. The charge density (DFT-D2) for the planes in the direction [001]. (a) the interaction between the adsorbate-substrate is negligible h=12Å , the charge distribution is uniform for each carbon atom of the graphene sheet. (b) adsorption between the molecule and graphene, the charge density show there are changes in distribution for graphene (c) overlap of charge density —molecule on graphene—.

Table 2. Charge transfer in the system graphene-histidine.

Approx	System	Net charge transferred to the molecule
LDA	Histidine	0.178 e
	Imidazole ring	0.076 e
GGA-PBE	Histidine	0.118 e
	Imidazole ring	0.023 e
DFT-D2	Histidine	0.188 e
	Imidazole ring	0.079 e

4. Conclusions

We studied the adsorption of histidine and imidazole ring on graphene using three approaches to the exchange and correlation interactions: LDA, GGA-PBE and DFT-D2. The calculations demonstrate that the adsorption energies satisfy the relation $E_{ads-DFT-D2} > E_{ads-LDA} > E_{ads-GGA-PBE}$. The adsorption distance for histidine meets the relation $d_{ads-DFT-D2} < d_{ads-LDA} < d_{ads-GGA-PBE}$, while for imidazole ring $d_{ads-LDA} < d_{ads-DFT-D2} < d_{ads-GGA-PBE}$. We reported the underestimation in adsorption energy and overestimation in adsorption distance in the approach GGA-PBE. We found a strong physisorption between histidine and graphene, when considering the van der Waals forces.

The interaction of histidine and the imidazole ring with graphene, showed signicant differences in the adsorption process when the carboxyl and amino groups were included, since their presence produces an important shift of the imidazole ring edge states towards E_F, improving eventual transport effects. For the three exchange and correlation schemes used, the adsorption energy was always lower in the imidazole ring system.

Also, there was a greater charge transfer from the graphene to histidine when the carboxyl and amino groups were included —0.18 e vs 0.07 e for the imidazole ring, from the approach DFT-D2—. All the studied substrate-adsorbate systems maintained the semi-metallic character (zero gap) of pure graphene.

The results suggests that graphene may be more sensitive when the adsorbed molecule includes carboxyl and amino groups. This information may be a useful guidance to develop novel graphene-based technology for the detection of amino acids.

References

[1] Neto A C, Guinea F, Peres N, Novoselov K and Geim A 2009 *Rev. Mod. Phys.* **81** 109–162
[2] Novoselov K, Geim A, Morozov S, Jiang D, Zhang Y, Dubonos S and Firsov A 2004 *Science* **306** 666–669
[3] Ferrari A 2014 *Nanoscale* **1** 1–343
[4] Yang Y, Asiri A, Tang Z, Du D and Lin Y 2013 *Materials Today* **16** 365–373
[5] Bellido E and Seminario J 2012 *J. Phys. Chem. C* **116** 8409–8416
[6] Wang Y, Zhaohui L, Dehong H, Chiann-Tso L, Jinghong L and Yuehe L 2010 *J. Am. Chem. .Soc.* **132** 9274–9276
[7] Hess L, Jansen M, Maybeck V, Hauf M, Seifert M, Stutzmann M, Sharp I, Offenhusser A and Garrido J 2011 *Advanced Materials* **23** 5045–5049
[8] Bendali A, Hess L, Seifert M, Forster V, Stephan A, Garrido J and Picaud S 2013 *Advanced Healthcare Materials* **2** 929–933
[9] Rajesh C, Majumder C, Mizuseki H and Kawazoe Y 2009 *J, Chem. Phys.* **76** 033401
[10] Lee E 2012 *Appl. Phys. Lett.* **100** 153117
[11] Gowtham S, Scheicher R, Ahuja R, RPandey and Karna S 2007 *Phys. Rev. B.* **76** 033401
[12] Berland K, Chakarova S, Cooper V, Langreth D and Schroder E 2010 *J. Phys.: Condens. Matter* **23** 135001
[13] Leenaerts O, Partoens B and Peerters F 2008 *Phys. Rev. B* **77** 125416
[14] Schedin F, AKGeim, Morozov S, Hill E, Blake P, Katsnelson M and Novoselov K 2007 *nature materials* **6** 652–655
[15] Lee J, Choi Y, Kim H, Scheicher R and Cho J 2013 *J. Phys. Chem. C* **117** 13435–13441
[16] Ortmann F, Schmidt W and Bechstedt F 2005 *Phys. Rev. Lett.* **95** 186101
[17] Woods L, Bdescu S and Reinecke T 2007 *Phys. Rev. B* **75** 155415
[18] Gowtham S, Scheicher R, RPandey, Karna S and Ahuja R 2008 *Nanotechnology* **19** 125701
[19] Ozaki T, Nishio K and Kino H 2010 *Phys. Rev. B* **81**
[20] Ozaki T 2003 *Phys. Rev. B.* **67** 155108
[21] Ozaki T and Kino H 2004 *Phys. Rev. B.* **69** 195113
[22] Perdew J P, Burke K and Ernzerhof M 1998 *Phys. Rev. Lett.* **80** 891

[23] Grimme S 2006 *J. Comp. Chem.* **27** 1787–1799
[24] Umadevi D and Sastry G 2013 *ChemPhysChem* **14** 2570–2578
[25] Vovusha H, Sanyal S and Sanyal B 2013 *J. Phys. Chem. Lett.* **4** 3710–3718
[26] Kokalj A 2003 *Comput. Mater. Sci.* **28** 155
[27] Momma K and Izumi F 2011 *J. Appl. Crystallogr.* **44** 1272